

Adaptive Identification and Control Algorithms for Nonlinear Bacterial Growth Systems*

D. DOCHAIN† and G. BASTIN†

Simple self-tuning type controllers for nonlinear bacterial growth processes can be effective and their stability can be proven under mild conditions.

Key Words—Adaptive control, fermentation processes, nonlinear systems, parameter estimation.

Abstract—This paper suggests how nonlinear adaptive control of nonlinear bacterial growth systems could be performed. The process is described by a time-varying nonlinear model obtained from material balance equations. Two different control problems are considered: substrate concentration control and production rate control. For each of these cases, an adaptive minimum variance control algorithm is proposed and its effectiveness is shown by simulation experiments. A theoretical proof of convergence of the substrate control algorithm is given. A further advantage of the nonlinear approach of this paper is that the identified parameters (namely the growth rate and a yield coefficient) have a clear physical meaning and can give, in real time, a useful information on the state of the biomass.

1. INTRODUCTION

A COMMONLY used approach for the adaptive control of nonlinear systems is to consider them as time-varying linear systems and to use black-box linear approximate models to implement the control law. This approach has been used by the authors in previous works on the control of fermentation processes (Bastin and coworkers, 1983a, b).

But, since the underlying process is nonlinear, improved control can be expected by exploiting the nonlinear structure of the model. Such an idea is pursued in the present paper: we suggest how nonlinear adaptive control of nonlinear bacterial growth systems can be implemented. A similar idea has recently been used for the dissolved oxygen adaptive control in waste water treatment (Ko, McInnis and Goodwin, 1982), but under a somewhat different form than in the present paper.

The process is described by a nonlinear state space representation obtained from usual material balance equations (Section 2). However, this representation does not require any specific analytical description of the bacterial growth rate.

The system is then approximated by a discrete-time time-varying model which is linear in the parameters and in the control input though globally nonlinear. The time-varying parameters in this model (namely the growth rate and a yield coefficient) have a clear physical meaning and are identified in real time with a standard RLS algorithm (Section 3).

The parameter estimation algorithm is combined with minimum-variance and Clarke–Gawthrop controllers to obtain adaptive controllers in two different cases: substrate concentration control (Section 4) and production rate control (Section 5). The effectiveness of the parameter estimation algorithm and the adaptive control algorithms is demonstrated by simulation experiments. Furthermore a theoretical proof of the convergence of the substrate control is given in the Appendix.

Parameter estimation and nonlinear control of microbial growth systems have been, in the last decade, the object of growing interest. Among many others, we may mention the papers by D'Ans, Kokotovic and Gottlieb (1971), Aborhey and Williamson (1978), Holmberg and Ranta (1982) and a large number of papers (and references) contained in the proceedings of the first IFAC Workshop on Modelling and Control of Biotechnical Processes (Halme, 1983), especially the contributions of Marsili-Libelli (1983) and Stephanopoulos and Ka-Yiu San (1983). However, we believe that the algorithms proposed in this paper have some original features that we can summarize as follows:

- (a) In our approach, the parameter estimation and the process control are performed *simultaneously*.

* Received 20 October 1983; revised 20 March 1984. The original version of this paper was presented at the IFAC Workshop on Adaptive Systems in Control which was held in San Francisco, California, U.S.A. during June 1983. The published proceedings of this IFAC meeting may be ordered from Pergamon Press Ltd, Headington Hill Hall, Oxford OX3 0BW, U.K. This paper was recommended for publication in revised form by associate editor P. Parks under the direction of editor B. Anderson.

† Laboratoire d'Automatique, de Dynamique et d'Analyse des Systèmes, University of Louvain, Bâtiment Maxwell, B-1348 Louvain-la-Neuve, Belgium.

- (b) The specific growth rate is not modelled by an analytical function of the state but is considered as a time-varying unknown parameter estimated in real time by a simple least-squares algorithm.
- (c) The control is performed by a very simple self-tuning scheme which contrasts with more sophisticated approaches followed elsewhere like, e.g. nonlinear optimal control (D'Ans, Kokotovic and Gottlieb, 1971), nonlinear state feedback with Riemannian geometric model (Takamatsu, Shioya and Kurome, 1983) or adaptive multimodel control (Cheruy, Panzarella and Denat, 1983).
- (d) Global convergence of the substrate control algorithm is established under mild conditions.

2. DESCRIPTION OF THE SYSTEM

We consider the usual state-space representation of bacterial growth systems by mass-balance equations

$$\begin{aligned} \dot{X} &= [\mu(X, S) - U] X \\ \dot{S} &= -k_1 \mu(X, S) X + U(V - S) \\ Y &= k_2 \mu(X, S) X \end{aligned} \quad (1)$$

with state variables:	X biomass concentration
	S substrate concentration
inputs:	U dilution rate (i.e. influent flow rate)
	V influent substrate concentration
outputs:	S substrate concentration
	Y production rate of the reaction product
parameters:	$\mu(X, S)$ growth rate
	k_1 and k_2 yield coefficients.

We could think of adopting an analytical expression for the bacterial growth rate $\mu(X, S)$; the most popular expression is certainly the Monod law

$$\mu(X, S) = \frac{\mu^* S}{K_m + S} \quad (\text{Monod}) \quad (2)$$

but many other expressions have been suggested, like

$$\mu(X, S) = \frac{\mu^* S}{K_b} \quad S \leq K_b \quad (\text{Blackman}) \quad (3)$$

$$\mu^* \quad S \geq K_b$$

$$\mu(X, S) = \frac{\mu^* S}{K_c X + S} \quad (\text{Contois}) \quad (4)$$

$$\mu(X, S) = \frac{\mu^* K_0 S}{1 + K_1 S + K_2 S^2} \quad (\text{Haldane}). \quad (5)$$

In these expressions, μ^* is the maximum growth rate.

The choice of an appropriate model for $\mu(X, S)$ is far from being an easy task and is the matter of continuing research (e.g. Roques and co-workers, 1982). Spriet (1982) lists no less than nine different models for $\mu(X, S)$ which have been proposed in the literature without even mentioning those which involve inhibitions (like the Haldane law (5)) or a pH-dependence (e.g. Vandenberg and coworkers, 1976).

Furthermore, it is well known that important identifiability difficulties occur when estimating the parameters (μ^* and K_m or K_b or $K_c \dots$) from real-life data (e.g. Holmberg and Ranta, 1982; Bastin and coworkers, 1983b, Holmberg, 1983).

Therefore we prefer to 'short-circuit' the problem of this choice and to identify the time-varying growth rate $\mu(X, S)$ in real-time by an adaptive algorithm.

Throughout this paper, we shall assume that:

- (a) the dilution rate U is the *control* input;
- (b) the influent substrate concentration V is an external *measurable* disturbance input;
- (c) the substrate concentration S and the production rate Y are *measurable* outputs.

A typical example: the anaerobic digestion process

The state-space representation (1) is suited to describe the methanization stage in an anaerobic digestion process. The anaerobic digestion can be used, for instance, for the treatment of wastes in sugar industries: U is the influent acetic acid concentration (i.e. the input pollution level), S is the output pollution level and Y is a methane gas flow rate. V and S are observed through BOD measurements. The main interest of such a water treatment plant is obviously to yield methane gas which can be used as an auxiliary energy supply. Further details on the anaerobic digestion process can be found in Antunes and Installé (1981), Van den Heuvel and Zoetmeyer (1982), and Bastin and coworkers (1983a, b).

3. ADAPTIVE PARAMETER ESTIMATION

Using a first-order Euler approximation for \dot{X} and \dot{S} , with a sampling period T , the following discrete-time equations are derived from the system equations (1)

$$\begin{aligned} X_{t+1} &= X_t + T\mu_t X_t - T U_t X_t + \tilde{v}_t \\ S_{t+1} &= S_t - T k_1 \mu_t X_t + T U_t (V_t - S_t) + \omega_t \\ Y_t &= k_2 \mu_t X_t. \end{aligned} \quad (6)$$

In these equations, the subscript t is a discrete-time index ($t = 0, 1, 2, \dots$) and the growth rate μ_t is a compact notation for $\mu_t = \mu(X_t, S_t)$.

We make the approximation

$$Y_{t+1} - Y_t = k_2 \mu_t (X_{t+1} - X_t) + \varepsilon_t. \quad (7)$$

Then, substituting for X_t and X_{t+1} from (7) into (6), we have

$$Y_{t+1} = Y_t + \mu_t T Y_t - T U_t Y_t + v_t \quad (8)$$

$$S_{t+1} = S_t + k T Y_t + T U_t (V_t - S_t) + \omega_t \quad (9)$$

with

$$v_t = \varepsilon_t + k_2 \mu_t \tilde{v}_t$$

$$k = -\frac{k_1}{k_2}$$

Equations (8) and (9) constitute the *basic discrete-time model* for the derivations of the parameter estimation and adaptive control algorithms. In this model, v_t and ω_t represent errors due to noise, discretization and approximation (7).

Since the basic model is linear in the parameters μ_t and k , recursive least-squares estimates can be readily obtained

$$\hat{\mu}_{t+1} = \hat{\mu}_t + T P_t Y_t (Y_{t+1} - Y_t + T U_t V_t - \hat{\mu}_t T Y_t) \quad (10)$$

$$\hat{k}_{t+1} = \hat{k}_t + T P_t Y_t (S_{t+1} - S_t - T U_t (V_t - S_t) - \hat{k}_t T Y_t) \quad (11)$$

$$P_t = \frac{P_{t-1}}{\lambda} \left(1 - \frac{T^2 Y_t^2 P_{t-1}}{\lambda + T^2 Y_t^2 P_{t-1}} \right)$$

with $P_0 \gg 0$ and $0 < \lambda \leq 1$.

λ is a forgetting factor to allow the tracking of the time-varying growth rate μ_t . This forgetting factor is also used for the estimation of the yield coefficient k to allow for variations 'due to unobservable physiological or genetic events' (Holmberg and Ranta, 1982). Notice that the estimation of both parameters is decoupled but with a common gain P_t .

In addition to these parameter estimates, the biomass concentration X can be estimated in real-time by writing $\hat{X}_t = Y_t / k_2 \hat{\mu}_t$.

Simulation results

Simulation experiments have been performed using state equations (1) as the 'true' bacterial growth system, with a Monod growth rate (2). The following parameters and initial state values were used:

$$\mu^* = 0.4 \quad K_m = 0.4 \quad k = -0.3636$$

$$X_0 = 0.069 \quad S_0 = 0.13.$$

The initial values of both estimated parameters $\hat{\mu}_t$ and \hat{k}_t were set to zero. These values will be used for all the simulation experiments throughout the

paper. Figure 1 shows the estimates $\hat{\mu}_t$ and \hat{k}_t computed by the algorithm equations (10) and (11) with $P_0 = 10^6 I$ and white noise input signals U_t and V_t .

The same experiment is shown in Fig. 2, except that a jump is applied on the maximum growth rate ($\mu^* = 0.4 \rightarrow 0.45$) at time $t = 240$.

We observe a fast convergence, without bias, of the parameter estimate \hat{k}_t and a slower convergence of $\hat{\mu}_t$ to the 'true' time-varying growth rate μ_t .

4. SUBSTRATE CONTROL

We consider the problem of regulating the substrate concentration S_t at a prescribed level S^* despite the disturbance input V_t , by acting on the dilution rate U_t .

In the anaerobic digestion example mentioned above, this is a depollution control problem with V_t and S_t the input and output pollution levels respectively.

A discrete-time minimum variance adaptive controller is adopted. At each sampling time, the control input U_t is computed by setting a one-step ahead prediction of the substrate concentration equal to the prescribed level

$$\hat{S}_{t+1} = S^*. \quad (12)$$

From the basic model equation (9), it is natural to define \hat{S}_{t+1} as follows:

$$\hat{S}_{t+1} = S_t + \hat{k}_t T Y_t + T U_t (V_t - S_t) \quad (13)$$

here \hat{k}_t is updated by the parameter estimation algorithm (11).

A nonlinear control law is readily obtained from (12), since \hat{S}_{t+1} is linear in U_t ; in practice, the control action U_t is obviously constrained by the operating conditions. Therefore, the adaptive control algorithm is as follows:

$$\bar{U}_t = \frac{S^* - S_t - \hat{k}_t T Y_t}{T(V_t - S_t)}$$

$$U_t = 0 \text{ if } \bar{U}_t < 0 \quad (14)$$

$$\bar{U}_t = U_{\max} \text{ if } \bar{U}_t > U_{\max}$$

$$U_t = \bar{U}_t \text{ otherwise.}$$

A block diagram of the closed-loop system is presented in Fig. 3. We note that a feedforward compensation of the measurable perturbation V_t is included.

Simulation results

Successful simulation experiments have been carried out, using the continuous-time state equations (1) as the 'true' system with a Monod growth rate (2) and $U_{\max} = 0.39$.

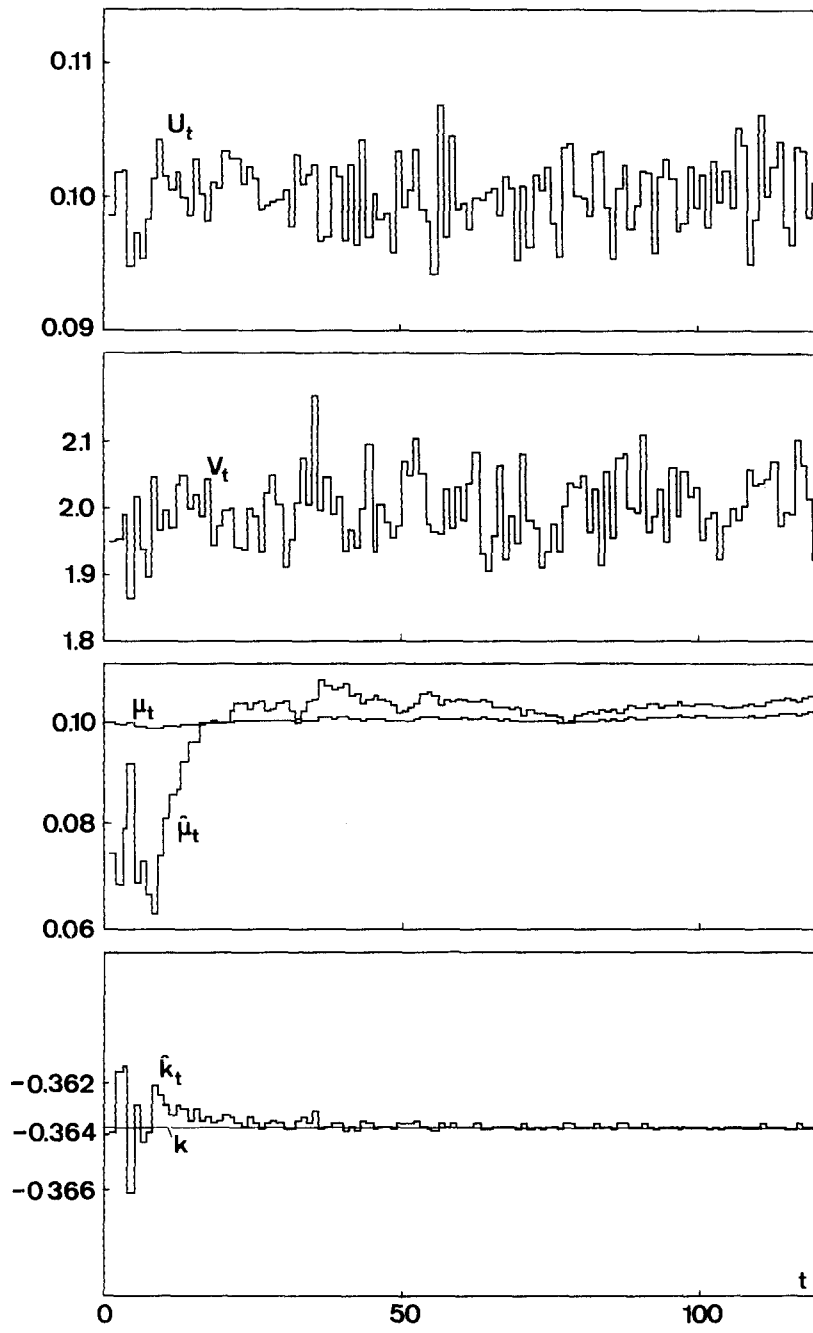


FIG. 1. Parameter estimation with white noise inputs.

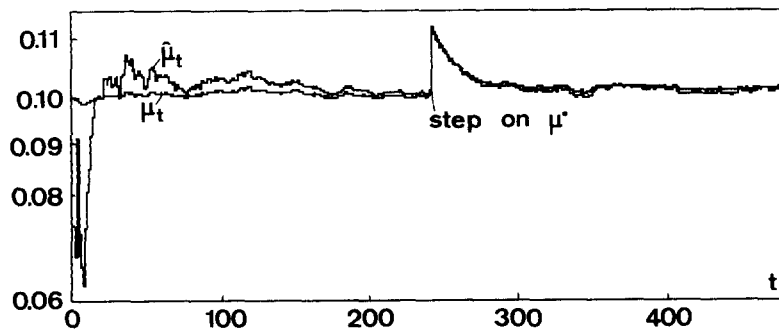


FIG. 2. Estimation of $\hat{\mu}_t$ with a step on μ^* at $t = 240$ s.

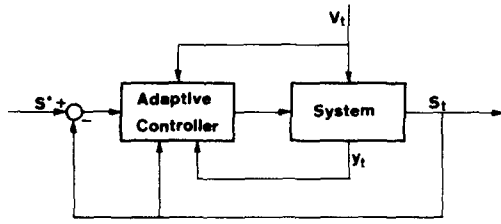


FIG. 3. Block diagram of the substrate concentration control.

Figure 4 shows the substrate concentration S_t , the control input U_t and the parameter estimates $\hat{\mu}_t$ and \hat{k}_t in the case of a square-wave set point with a period of 96 sampling times and a constant perturbation $V_t = 2$. We observe that the controlled output S_t ,

converges much faster than the parameter estimate $\hat{\mu}_t$, but this is not surprising since $\hat{\mu}_t$ is not actually used by the control algorithm.

Figure 5 shows the substrate concentration S_t , the control input U_t and the parameter estimates $\hat{\mu}_t$ and \hat{k}_t in the case of a square-wave perturbation V_t and an additive white noise on the auxiliary output Y . Evidently, we observe a bias (due to the noise) in the parameter estimates but this is not important for the convergence of controlled output S_t .

Figure 6 shows the substrate concentration S_t and the control input U_t in the case of a 10% square-wave variation of the maximum growth rate.

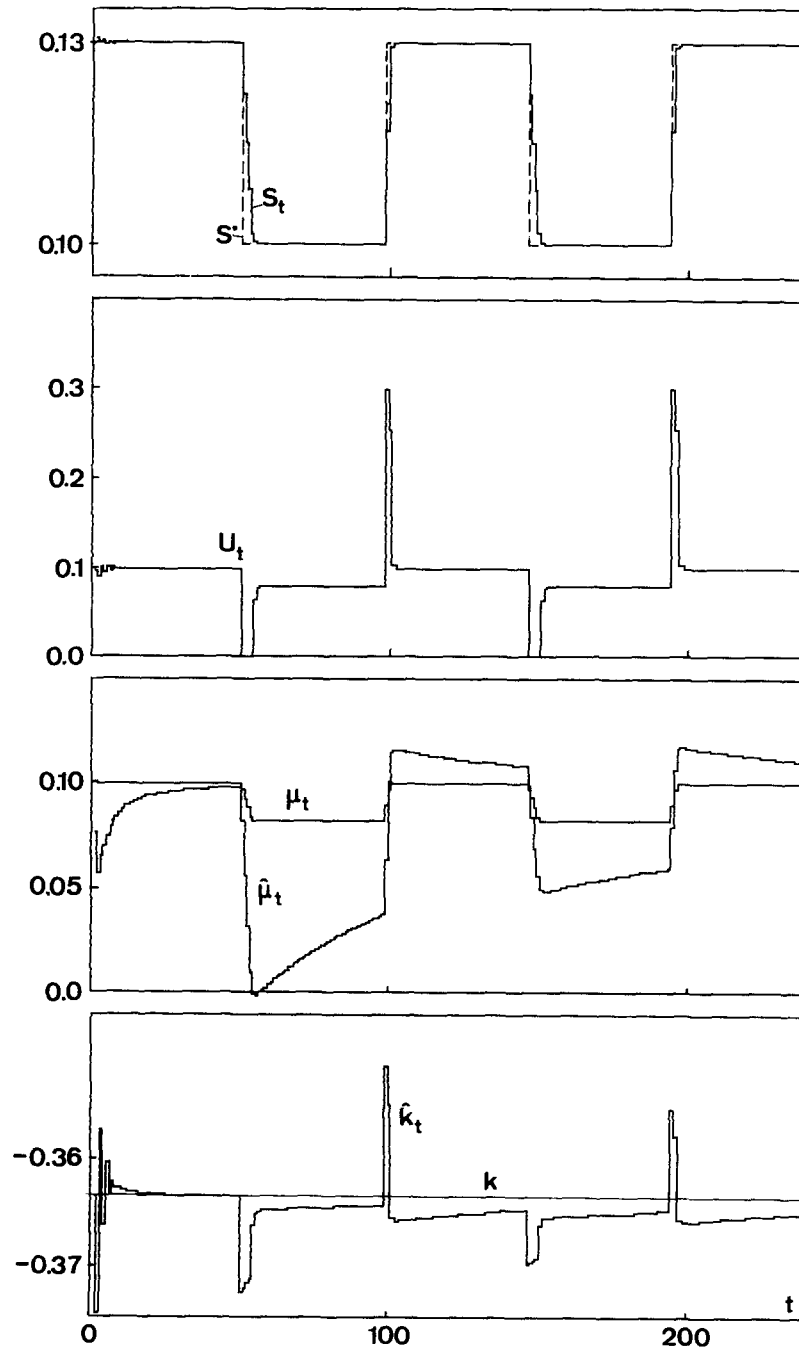


FIG. 4. Substrate concentration control with a square-wave set point.

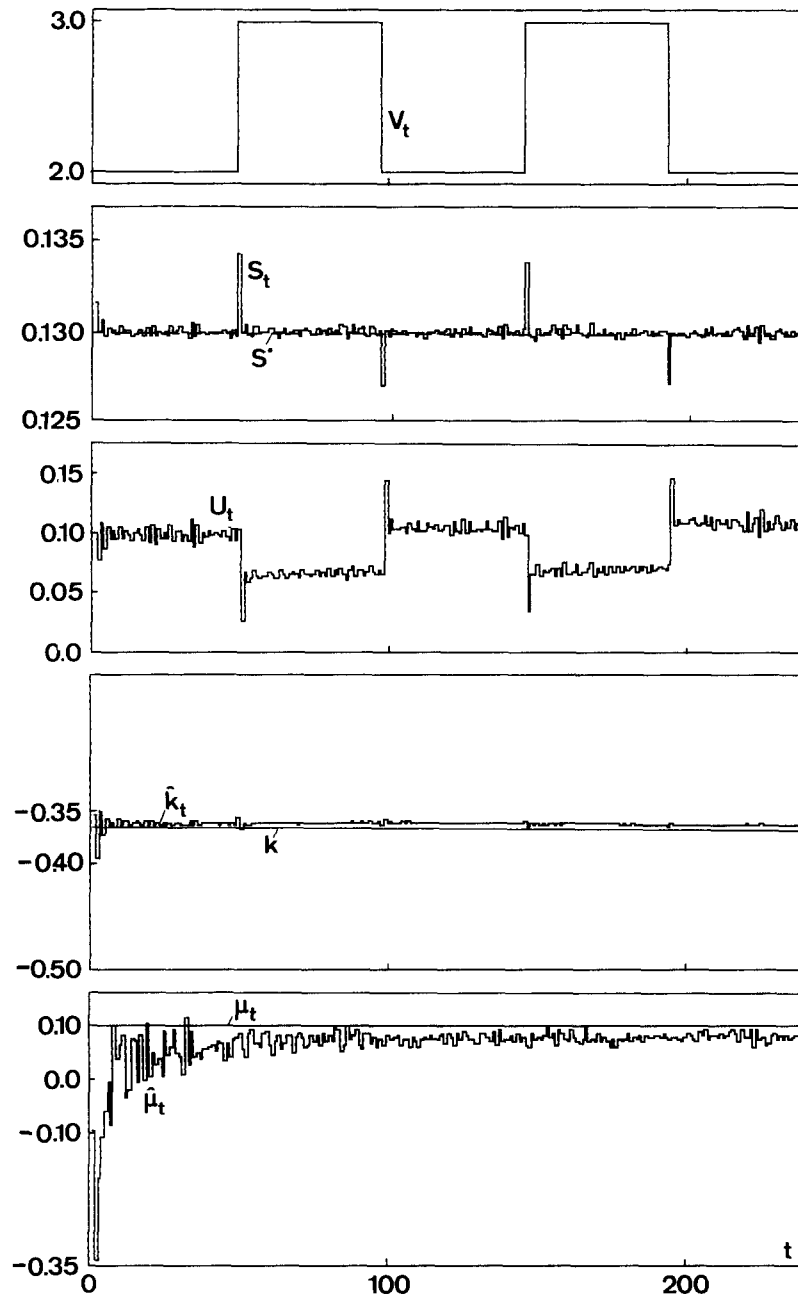


FIG. 5. Substrate concentration control with a square-wave input perturbation.

5. PRODUCTION RATE CONTROL

In order to facilitate the understanding of the later discussions, we refer here to the particular case of the anaerobic fermentation process described in Section 2 but, obviously, the results can also apply to other processes with the same structure.

The anaerobic digestion can be viewed as an energy conversion process. An amount of 'organic' energy is available in the influent under the form of the input organic load V_t . This energy is converted into methane gas Y_t by the anaerobic digestion. Obviously, the output energy Y_t cannot, in the mean, be larger than the available input energy. When the aim of the plant is not depollution but energy

production (as in industrial farms), the control objective is to continuously adapt the output production Y_t to the available input load V_t . Therefore, the desired gas production Y_t^* is defined as follows:

$$Y_t^* = \beta V_t - \beta_0 \quad \beta > 0, \quad \beta_0 > 0. \quad (15)$$

The coefficients β and β_0 have to be selected carefully by the user since if, by lack of knowledge, β is chosen too large or β_0 too small (i.e. if we require from the fermentor more methane gas than it can actually provide) then the process can be driven by the controller to a wash-out steady-state (Antunes

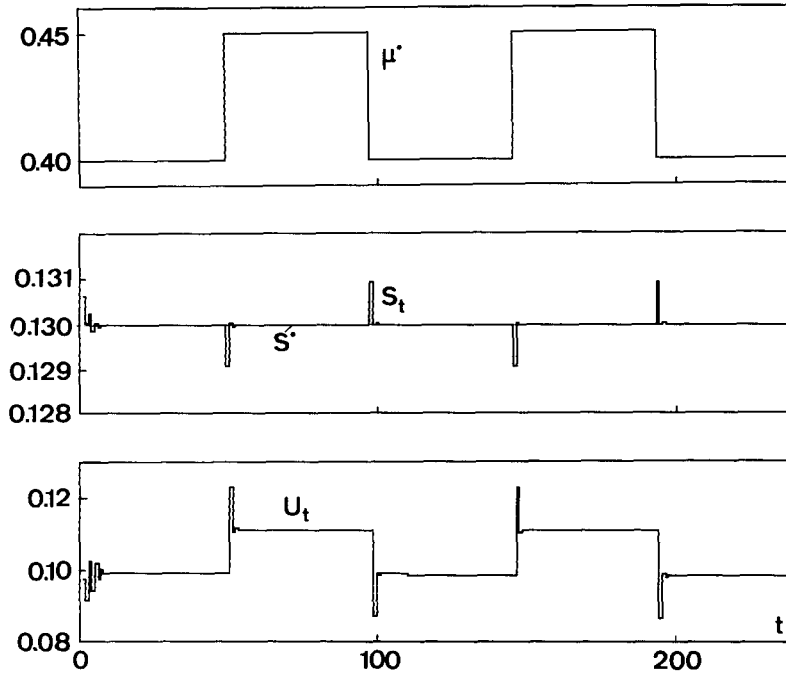


FIG. 6. Substrate concentration control with a square-wave perturbation on μ^* .

and Installé, 1981), i.e. to a state where the bacterial life has completely disappeared and where the reactor is definitely stopped.

In this section, we shall first demonstrate that a minimum variance adaptive control law using the basic model equation (8) may diverge. We shall then describe what kind of modification we bring to the model in order to improve the control algorithm.

Divergence of the minimum variance controller

As for the substrate concentration control, we first try to use a minimum variance control law derived from the basic model equation (8)

$$\begin{aligned} \bar{U}_t &= -\frac{Y_{t+1}^* - Y_t(1 + T\hat{\mu}_t)}{TY_t} \\ U_t &= 0 \text{ if } \bar{U}_t < 0 \\ U_t &= U_{\max} \text{ if } \bar{U}_t > U_{\max} \\ U_t &= \bar{U}_t \text{ otherwise.} \end{aligned} \quad (16)$$

Consider the case when $Y_{t+1}^* > Y_t(1 + T\hat{\mu}_t)$. Then $\bar{U}_t < 0$, i.e. U_t is set to zero.

If U_t is kept equal to zero, Y_t , possibly after a transient increasing period, will decrease and tend to zero (gas can no longer be produced if the influent has disappeared!). So, if the transient on Y_t is not important enough, U_t remains at the zero value, and Y_t tends to zero.

Figure 7 illustrates this feature: at time $t = 48$,

the desired output level Y_{t+1}^* is set to a value 15% larger than the steady-state value of Y_t .

Modification of the basic discrete-time model

In order to improve the control algorithm, we introduce the following modifications of the basic model equations.

First, we consider the following approximate relation between μ and S :

$$\mu(X, S) = b(X, S)S \quad (17)$$

i.e. the parameter b is estimated, instead of μ , with a recursive least-square algorithm.

One may consider this approximation as a loss of generality with respect to the previous case where μ is left independent of any analytical expression and estimated as a parameter of the system. But this is plainly justified by the fact that all the proposed bacterial growth laws are compatible with (17).

Rewrite the expression of Y_t from (6)

$$Y_t = k_2 b_t S_t X_t$$

We modify the approximation (7) by the following one:

$$Y_{t+1} - Y_t = k_2 b_t [S_t(X_{t+1} - X_t) + X_t(S_{t+1} - S_t)] + \epsilon_t \quad (18)$$

i.e. the variation $\Delta Y_t = Y_{t+1} - Y_t$ is now dependent on both the variations ΔX_t in the bacterial

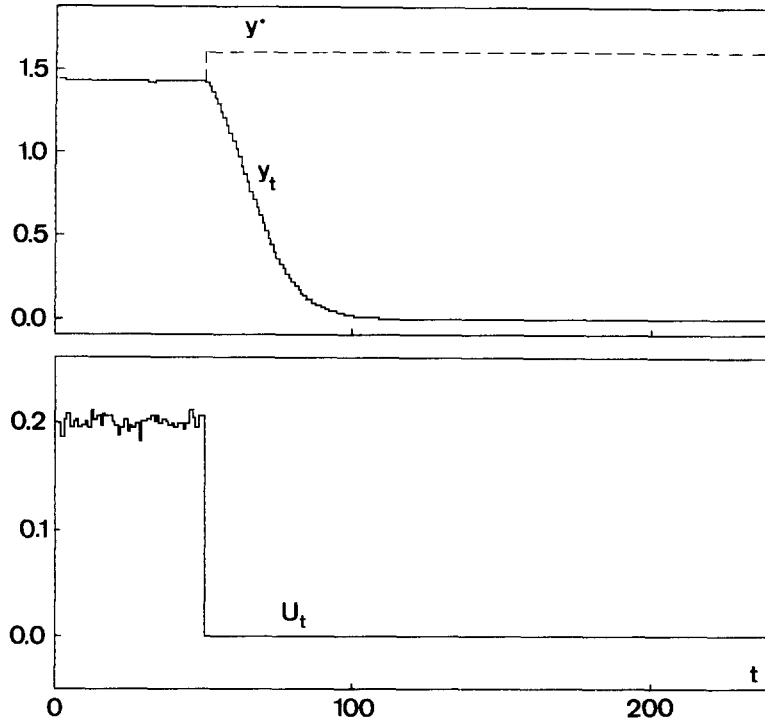


FIG. 7. Production rate control: divergence of a simple MV controller.

concentration and ΔS_t in the substrate concentration. Equation (8) becomes

$$Y_{t+1} = Y_t + b_t T S_t Y_t + k T \frac{Y_t^2}{S_t} + T U_t Y_t \left(\frac{V_t}{S_t} - 2 \right) + v_t \quad (19)$$

with $v_t = \varepsilon_t + k_2 b_t S_t \tilde{v}_t + k_2 b_t X_t \omega_t$.

Since (19) is linear in the parameter b_t , recursive least-squares estimates can be obtained

$$\hat{b}_{t+1} = \hat{b}_t + T S_t Y_t P'_t (Y_{t+1} - Y_t - \hat{k}_t T \frac{Y_t^2}{S_t} + T U_t Y_t \left(\frac{V_t}{S_t} - 2 \right) - \hat{b}_t T S_t Y_t) \quad (20)$$

$$P'_t = \frac{P'_{t-1}}{\lambda} \left(1 - \frac{T^2 Y_t^2 S_t^2 P'_{t-1}}{\lambda + T^2 Y_t^2 S_t^2 P'_{t-1}} \right) \quad (21)$$

In these expressions the value of \hat{k}_t is assumed to be estimated by the recursive least-squares equation (11).

Notice that parameters \hat{k}_t and \hat{b}_t are estimated 'in cascade'. This allows us to decouple the estimation of both parameters, and to keep a very simple scalar identification algorithm.

Figure 8 shows the same experiment as Fig. 1, but for the estimation of \hat{b}_t .

New minimum variance control algorithm

As above, we choose a discrete-time minimum variance adaptive controller. Using (19), the control input U_t is given by

$$\bar{U}_t = \frac{Y_{t+1}^* - Y_t - T \hat{k}_t Y_t^2 / S_t - T \hat{b}_t S_t Y_t}{T Y_t (V_t / S_t - 2)} \quad (22)$$

$$U_t = 0 \quad \text{if } \bar{U}_t < 0$$

$$U_t = U_{\max} \quad \text{if } \bar{U}_t > U_{\max}$$

$$U_t = \bar{U}_t \quad \text{otherwise.}$$

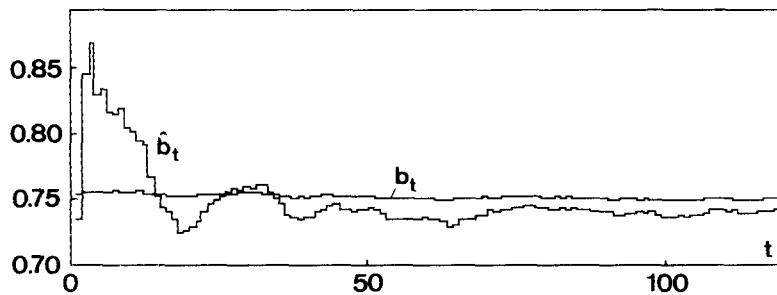


FIG. 8. RLS estimation of b_t .

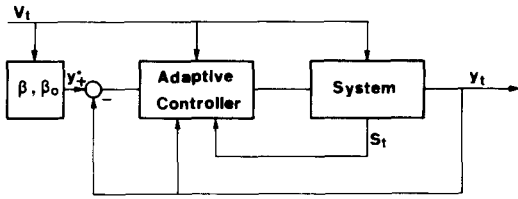


FIG. 9. Block diagram of the production rate control.

A block diagram of the closed-loop system is presented in Fig. 9.

Simulation results

The minimum variance adaptive controller, as written in (22), is more effective than the previous one (16). As a comparison, Fig. 10 shows the same experiment as Fig. 7, but with the control law (22).

In Fig. 11 steps of the influent substrate concentration V_t (external measurable perturbation), i.e. of the desired output level Y_t^* (see (15)), are applied to the system.

The control algorithm converges very quickly, although the convergence of the parameter \hat{b}_t to its 'true' time-varying value is much slower.

Clarke-Gawthrop controller

It is evident, from (22), that the sign of \bar{U}_t depends on the sign of $(V_t/S_t - 2)$. When the substrate concentration S_t reaches values close to $0.5 V_t$, the minimum variance controller may appear not to be able to reach the desired set point. If S_t is larger than $0.5 V_t$, \bar{U}_t becomes negative, i.e. $U_t = 0$. As a consequence, S_t decreases. When S_t becomes smaller than $0.5 V_t$, \bar{U}_t is set to a positive value. If $(V_t/S_t - 2)$

is close to zero, \bar{U}_t most likely reaches large values, larger than U_{max} , and S_t increases again so that $(V_t/S_t - 2)$ becomes negative, and so on.

In such a case, U_t is oscillating between 0 and U_{max} , leading to the oscillation of the system, and the control does not converge. A typical illustration is given in Fig. 12.

In order to solve these convergence problems, we introduce a Clarke-Gawthrop (1979) control law using a weight $Q(1 - z^{-1})$ in the performance index (Belanger, 1983). The control input is then computed so as to minimize the following criterion:

$$J = (\hat{Y}_{t+1} - Y_{t+1}^*)^2 + Q^2(U_t - U_{t-1})^2. \quad (23)$$

Using (19), we have

$$\bar{U}_t = \frac{Q^2}{Q^2 + T^2 Y_t^2 (V_t/S_t - 2)^2} U_{t-1} + \frac{T Y_t (V_t/S_t - 2)}{Q^2 + T^2 Y_t^2 (V_t/S_t - 2)^2} \left[Y_{t+1}^* - Y_t - \hat{k}_t T \frac{Y_t^2}{S_t} - \hat{b}_t T S_t Y_t \right]. \quad (24)$$

Figure 13 shows the improvement obtained by using this Clarke-Gawthrop controller. It is interesting to note that, as above, the convergence of the controlled output Y_t (Fig. 13) is much faster than the convergence of the parameter estimates (Fig. 14).

6. CONCLUSIONS

Simple adaptive controllers for a class of biotechnical systems have been proposed. Their

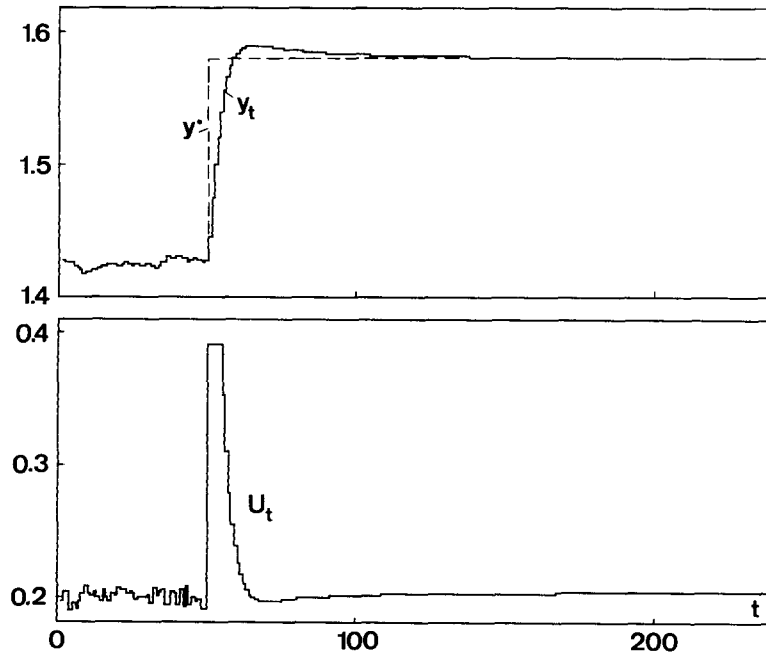


FIG. 10. Production rate control: convergence of the modified MV controller.

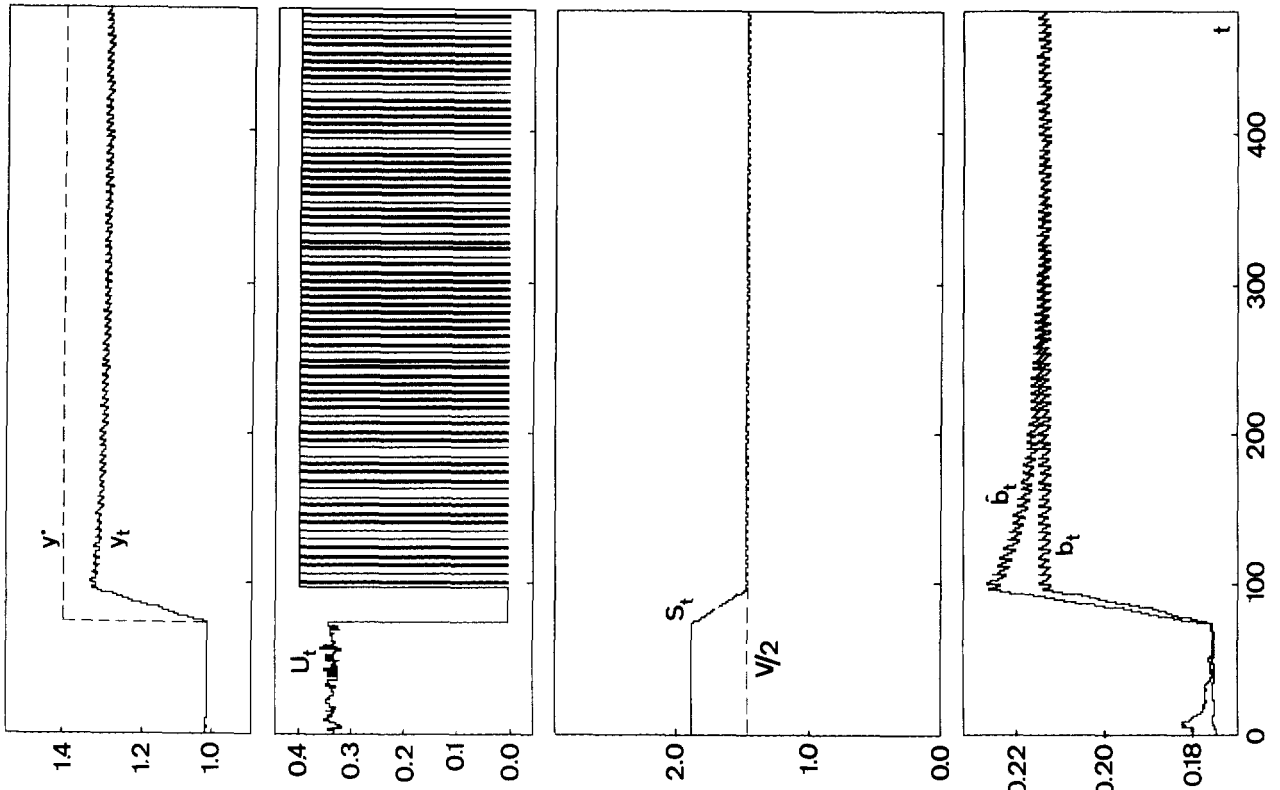


FIG. 12. Oscillation of the modified MV controller.

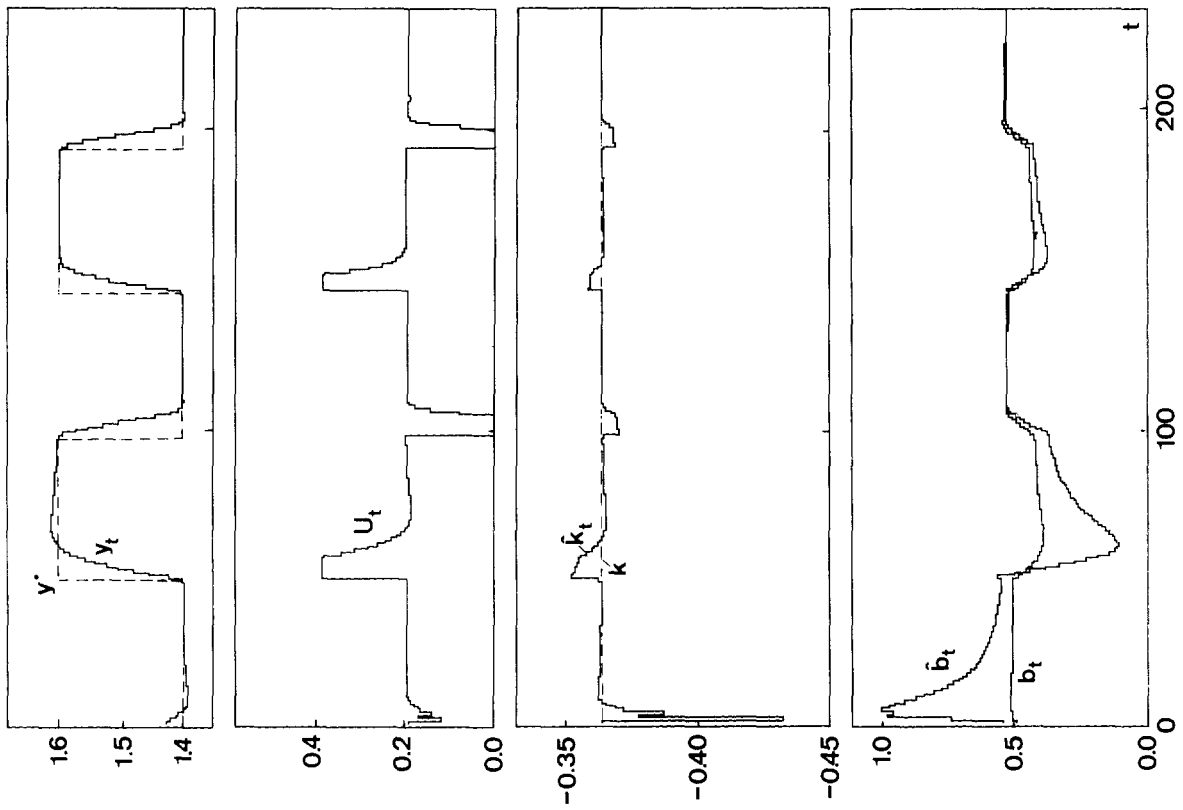


FIG. 11. Production rate control with a square-wave set point.

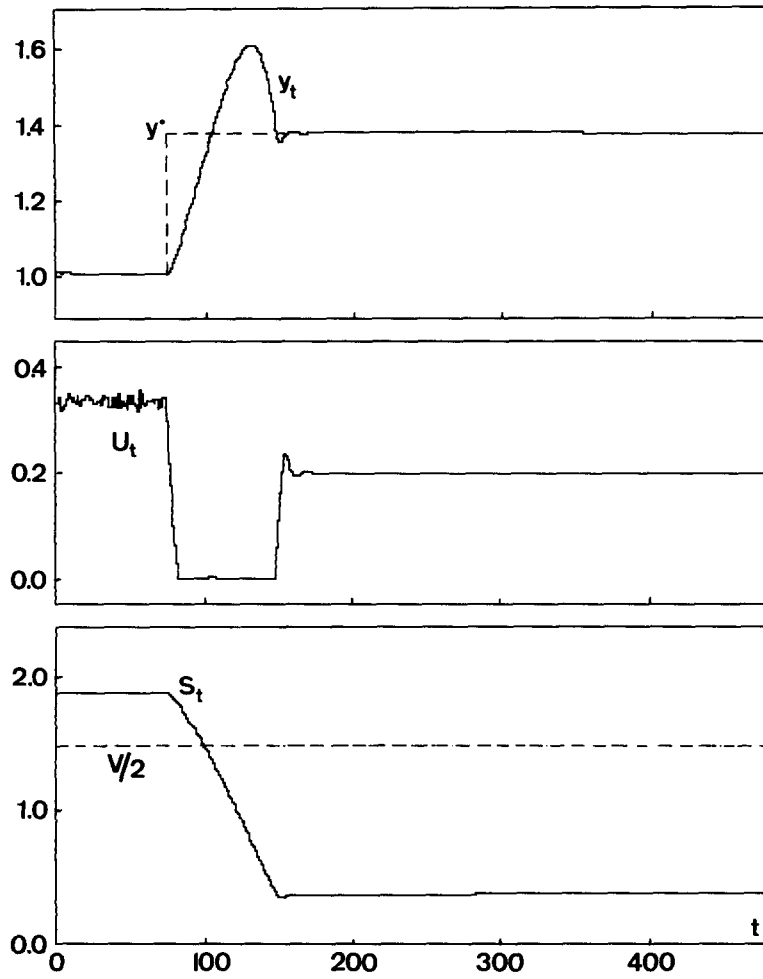


FIG. 13. Production rate control with a CG controller.

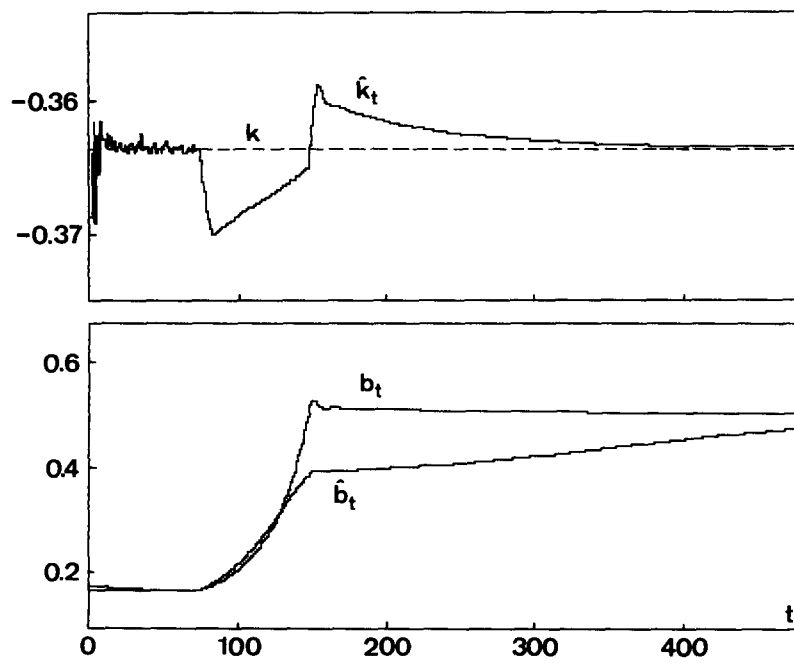


FIG. 14. Production rate control: evolution of the parameter estimates.

effectiveness has been demonstrated by simulation experiments.

A theoretical proof of the convergence of substrate concentration control algorithm is given in the Appendix. In the case of production rate control, the convergence of the algorithm has not been discussed and is obviously much more difficult to establish since the algorithm involves two cascaded steps together with the estimation of a truly time-varying parameter (μ_t).

In addition to the control itself, a further advantage of the nonlinear approach of this paper is that the identified parameters correspond clearly to physical parameters (namely growth rate and yield coefficient); therefore they can provide useful information, in real-time, on the state of the biomass.

Although the model (1) is well suited to industrial applications like waste treatment in sugar industries, in many other applications the model (1) is only the last stage of a complex multistage reaction: a typical situation is a five-state twelve parameter model (e.g. Bastin and coworkers, 1983b) describing a sequence of three reactions (solubilization, acidification, methanization). This is a further reason to explore the possibility of simple control schemes for the different stages of such high-order highly nonlinear systems.

Acknowledgements—The authors wish to thank M. I. Installé from the Laboratory of Automatic Control (University of Louvain), H. Naveau, E. J. Nyns and D. Poncelet from the Laboratory of Biotechnology (University of Louvain), A. Cheruy and L. Dugard from the Laboratory of Automatic Control (ENSIEG, Grenoble) for fruitful discussions about this work.

REFERENCES

- Aborhey, S. and D. Williamson (1978). State and parameter estimation of microbial growth processes. *Automatica*, **14**, 493–498.
- Antunes, S. and M. Installé (1981). The use of phase-plane analysis in the modelling and the control of a biomethanization process. *Proceedings of the 8th IFAC World Congress*, Kyoto, Japan, Vol. XXII, pp. 165–170.
- Bastin, G., D. Dochain, M. Haest, M. Installé and P. Opdenacker (1983a). Modelling and adaptive control of a continuous anaerobic fermentation process. In *Modelling and Control of Biotechnical Processes*, A. Halme (ed). Pergamon Press, Oxford, pp. 299–306.
- Bastin, G., D. Dochain, M. Haest, M. Installé and P. Opdenacker (1983b). Identification and adaptive control of a biomethanization process. In *Modelling and Data Analysis in Biotechnology and Medical Engineering*, G. C. Vansteenkiste and P. C. Young (eds). North-Holland, New York, pp. 271–282.
- Belanger, P. R. (1983). On type I systems and the Clarke-Gawthrop regulator. *Automatica*, **19**, 91–94.
- Cheruy, A., L. Panzarella and J. P. Denat (1983). Multimodel simulation and adaptive stochastic control of an activated sludge process. In *Modelling and Control of Biotechnical Processes*, A. Halme (ed). Pergamon Press, Oxford, pp. 127–183.
- Clarke, D. W. and P. J. Gawthrop (1979). Self-tuning control. *Proc. IEEE*, **126**, 633–640.
- D'Ans, G., P. V. Kokotovic and D. Gottlieb (1971). A nonlinear regulator problem for a model of biological waste treatment. *IEEE Trans. Aut. Control*, **AC-16**, 341–347.
- Goodwin, G. C., B. McInnis and R. S. Long (1982). Adaptive control algorithms for waste water treatment and pH neutralization. *Opt. Control Appl. Meth.* **3**, 443–459.
- Goodwin, G. C. and K. S. Sin (1983). *Adaptive Filtering Prediction and Control*. Prentice-Hall, Englewood Cliffs, NJ.
- Halme, A. (1983). Modelling and control of biotechnical processes. *Proceedings of the 1st IFAC Workshop*, Helsinki, Finland, 17–19 August 1982. Pergamon Press, Oxford.
- Holmberg, A. (1983). On the accuracy of estimating in the parameters of models containing Michaelis–Menten type nonlinearities. In *Modelling and Data Analysis in Biotechnology and Medical Engineering*, G. C. Vansteenkiste and P. C. Young (eds). North-Holland, New York, pp. 199–208.
- Holmberg, A. and J. Ranta (1982). Procedures for parameter and state estimation of microbial growth process models. *Automatica*, **13**, 181–193.
- Ko, K. Y., B. C. McInnis and G. C. Goodwin (1982). Adaptive control and identification of the dissolved oxygen process. *Automatica*, **18**, 727–730.
- Marsili-Libelli, S. (1983). On-line estimation of bioactivities in activated sludge processes. In *Modelling and Control of Biotechnical Processes*, A. Halme (ed). Pergamon Press, Oxford, pp. 121–126.
- Roques, H., S. Yve, S. Saipanich and B. Capdeville (1982). Is Monod's approach adequate for the modelisation of purification processes using biological treatment? *Water Resources*, **16**, 839–847.
- Spriet, J. A. (1982). Modelling of the growth of micro-organisms: a critical appraisal. In *Environmental Systems Analysis and Management*, Rinaldi (ed). North-Holland, New York, pp. 451–456.
- Stephanopoulos, G. and Ka-Yiu San (1983). On-line estimation of time-varying parameters: application to biochemical reactors. *Modelling and Control of Biotechnical Processes*, A. Halme (ed). Pergamon Press, Oxford, pp. 195–199.
- Takamatsu T., S. Shioya and H. Kurome (1983). Dynamics and control of a mixed culture in an activated sludge process. *Modelling and Control of Biotechnical Processes*, A. Halme (ed). Pergamon Press, Oxford, pp. 103–109.
- Vandenberg, L., G. B. Patel, D. S. Clark and C. P. Lentz (1976). Factors affecting rate of methane formation from acetic acid by enriched methanogenic cultures. *Can. J. Microbiol.*, **22**, 1312–1319.
- Van den Heuvel, J. C. and R. J. Zoetmeyer (1982). Stability of the methane reactor: a simple model including substrate inhibition and cell recycle. *Process Biochemistry*, May–June, 14–19.

APPENDIX: CONVERGENCE ANALYSIS OF THE SUBSTRATE CONCENTRATION CONTROL ALGORITHM

In this Appendix, we present a proof of the convergence of the substrate concentration control under a set of reasonable assumptions.

The demonstration has some similarities with that proposed by Goodwin, McInnis and Long (1982) in the case of dissolved oxygen control for waste water treatment.

It is organized in three steps:

- BIBO stability of the bacterial growth system,
- convergence of the parameter estimation algorithm,
- convergence of the adaptive control algorithm.

BIBO stability of the continuous-time bacterial growth system

Let us rewrite, for convenience, the state-space description of the bacterial growth system

$$\dot{X} = [\mu(X, S) - U]X \quad (A1a)$$

$$\dot{S} = -k_1\mu(X, S)X + U(V - S) \quad (A1b)$$

$$Y = k_2\mu(X, S)X. \quad (A1c)$$

In this section we prove the BIBO stability of this system (in accordance with the physical situation) under the following assumptions.

Assumptions.

- (H1a) $0 \leq \mu(X, S) \leq \mu^*$
 (H1b) $\mu(X, 0) = 0$.

- (H2a) $0 \leq U \quad 0 \leq V \leq V_{\max}$
 (H2b) $0 \leq S(0) \quad 0 \leq X(0) \quad k_1 X(0) + S(0) \leq V_{\max}$.

Notice that all the growth rate models of Section 2 fulfill assumption (H1).

Lemma 1. Under assumptions (H1) and (H2)

- (i) $0 \leq S \leq V_{\max}$
 (ii) $0 \leq X \leq \frac{V_{\max}}{k_1}$ (A2)
 (iii) $0 \leq Y \leq \frac{k_2}{k_1} \mu^* V_{\max} \quad \forall t > 0$.

Proof.

- (1) $X \geq 0$ and $Y \geq 0$; straightforward by using (A1a), (A1c) and (H2b).
 (2) For $S = 0$, we have $S \geq 0$, using (H2a), (A1b) and (H1b). The conclusion $S \geq 0$ for all S follows from (H2b).
 (3) For $S = V_{\max}$, we have, using (A1b), (A1c) and (H2a).

$$\dot{S} = -\frac{k_1}{k_2} Y + U(V - V_{\max}) \leq 0 \text{ since } Y \geq 0. \quad (\text{A3})$$

The conclusion $S \leq V_{\max}$ for all S follows from (H2b).

- (4) Define the auxiliary variable $Z = k_1 X + S$. Then, the following equation is readily derived from (A1a) and (A1b):

$$\dot{Z} = U(V - Z). \quad (\text{A4})$$

For $Z = V_{\max}$, we have $\dot{Z} \leq 0$. The conclusion $Z \leq V_{\max}$ for all Z follows. Since $S \geq 0$, clearly we have $X \leq V_{\max}/k_1$ for all X and it becomes obvious that, by using (A1c) and (H1a),

$$Y \leq \frac{k_2}{k_1} \mu^* V_{\max}. \quad (\text{A5})$$

Q.E.D.

It should be emphasized that from Lemma 1, the outputs S and Y and the state X are bounded without imposing any upper bound on the input U .

Convergence of the parameter estimation algorithm

We consider now the convergence of the estimation algorithm for the parameter \hat{k}_i presented in Section 3.

The basic idea is due to Goodwin and Sin (1983) and can be roughly summarized as follows: if the noise term ω_t in (9) is bounded, then the convergence of the parameter estimate \hat{k}_i can be guaranteed by involving, in the algorithm, a switching function to hold the parameter estimate constant wherever the prediction error becomes smaller than a prespecified bound. The algorithm (11) is considered without the forgetting factor ($\lambda = 1$) and modified as follows:

$$\hat{k}_{i+1} = \hat{k}_i + \sigma_i T P_i Y_i (S_{i+1} - \hat{S}_{i+1}) \quad (\text{A6})$$

$$P_i = P_{i-1} \left(1 - \frac{\sigma_i T^2 Y_i^2 P_{i-1}}{1 + \sigma_i T^2 Y_i^2 P_{i-1}} \right) \quad P_0 > 0 \quad (\text{A7})$$

with \hat{S}_{i+1} defined by (13).

Assumptions.

- (H3) $\sup |\omega_t| \leq \Delta$ (A8)
 (H4) $\sigma_t = 1$ if $\frac{(S_{i+1} - \hat{S}_{i+1})^2}{1 + T^2 Y_i^2 P_{i-1}} > \Delta^2$ (A9)
 $\sigma_t = 0$ otherwise.

Lemma 2. For the algorithm (A6) and (A7), subject to assumptions (H1)–(H4), then

$$\limsup_{t \rightarrow \infty} |S_t - \hat{S}_t| \leq C\Delta \quad (\text{A10})$$

with C a positive constant independent of Δ .

Proof.

$$\text{Let } \tilde{k}_i = \hat{k}_i + \frac{k_1}{k_2}. \quad (\text{A11})$$

Then, the following expression is readily derived from (A6) and (13):

$$\frac{\tilde{k}_{i+1}}{P_i} = \frac{\tilde{k}_i}{P_{i-1}} + \sigma_i T Y_i \omega_i. \quad (\text{A12})$$

Then, by assumption (H4),

$$\frac{\tilde{k}_{i+1}^2}{P_i} - \frac{\tilde{k}_i^2}{P_{i-1}} \leq \left[\Delta^2 - \frac{(S_{i+1} - \hat{S}_{i+1})^2}{1 + \sigma_i T^2 Y_i^2 P_{i-1}} \right]. \quad (\text{A13})$$

Then, $\frac{\tilde{k}_i^2}{P_{i-1}}$ is a nonincreasing function, bounded below by zero (since $P_{i-1} > 0$) and

$$\lim_{t \rightarrow \infty} \sigma_t \left[\Delta^2 - \frac{(S_{i+1} - \hat{S}_{i+1})^2}{1 + \sigma_i T^2 Y_i^2 P_{i-1}} \right] = 0. \quad (\text{A14})$$

$$\text{Hence } \limsup_{t \rightarrow \infty} \left[\frac{(S_{i+1} - \hat{S}_{i+1})^2}{1 + \sigma_i T^2 Y_i^2 P_{i-1}} \right] \leq \Delta^2. \quad (\text{A15})$$

Now, from (A7), the sequence P_i converges and we define

$$P_\infty = \lim_{t \rightarrow \infty} P_t \geq 0. \quad (\text{A16})$$

Hence, in view of Lemma 1,

$$\lim_{t \rightarrow \infty} \sigma_t Y_t^2 P_{t-1} \leq T^2 \left(\frac{k_2}{k_1} \mu^* V_{\max} \right)^2 P_\infty = C^2 - 1 \quad (\text{A17})$$

and, from (A15),

$$\limsup_{t \rightarrow \infty} |S_{t+1} - \hat{S}_{t+1}| \leq C\Delta. \quad (\text{A18})$$

Convergence of the adaptive control algorithm

We consider now the adaptive control algorithm (14). We have the following convergence result.

Theorem.

- If (i) $V_{\min} \leq V \leq V_{\max}$
 (ii) $S^* < V_{\min}$
 (iii) the parameter estimation algorithm (A6) and (A7) and the adaptive control algorithm (14) are used with

$$U_{\max} \geq \frac{\mu^* V_{\max}}{V_{\min} - S^*} \quad (\text{A19})$$

- (iv) Assumptions (H1), (H2b), (H3) and (H4) hold

$$\text{then } \limsup_{t \rightarrow \infty} |S_t - S^*| \leq C\Delta \quad (\text{A20})$$

with C the same constant as in Lemma 2.

Proof. From Lemma 2, for each $\eta > 0$, there exists $t_0 > 0$ such that

$$\hat{S}_t - C\Delta - \eta \leq S_t \leq \hat{S}_t + C\Delta + \eta \text{ for all } t \geq 0. \quad (\text{A21})$$

Define the interval

$$I = [S^* - C\Delta - \eta, S^* + C\Delta + \eta]. \quad (\text{A22})$$

(1) If the control algorithm gives $0 < U_{t_0} < U_{\max}$ then $\hat{S}_{t_0+1} = S^*$ and hence $S_{t_0+1} \in I$.

(2) If the control algorithm gives $U_t = 0$ for $t = t_0 + k$ for $k = 0, 1, 2, 3, \dots$ then by definition of \bar{U}_t , we have $\hat{S}_{t_0+k} \geq S^*$ for $k = 1, 2, 3, \dots$ and hence $S_{t_0+k} \geq S^* - C\Delta - \eta$.

But, if $U_t = 0$, S_t decreases and tends asymptotically to the steady-state $S = 0$, and there exists k' such that $S_{t_0+k'} \leq S^* + C_3\Delta + \eta$. The conclusion $S_{t_0+k'} \in I$ follows.

If the sequence $U_{t_0+k'} = 0$ terminates at time $t' > t_0$ so that $S_{t'} \in I$ and $0 < U_{t'} < U_{\max}$, then $S_{t'+1} \in I$ as in (1) above.

(3) If the control algorithm gives $U_t = U_{\max}$ for $t = t_0 + k$, $k = 0, 1, 2, 3, \dots$ then S_t increases since $\dot{S} \geq 0$ by definition of U_{\max} and we can prove similarly that $S_{t_0+k} \in I$ or $S_{t'+1} \in I$.

(4) So far, we have shown that there exists some $t_1 > t_0$ such that $S_{t_1} \in I$. Now it is easy to show that, if $S_{t_1} \in I$, then $S_t \in I$ for all $t \geq t_1$, by using the arguments of (1)–(3) above.

Thus we have

$$|S_t - S^*| \leq C\Delta + \eta \text{ for all } t \geq t_1. \quad (\text{A23})$$

Since $\eta > 0$ may be chosen arbitrarily small, it follows from the definition of I :

$$\limsup_{t \rightarrow \infty} |S_t - S^*| \leq C\Delta. \quad (\text{A24})$$

Q.E.D.

Comments.

- (1) The controller achieves a zero steady-state error even with a varying disturbance V_t since the algorithm includes feedforward compensation.
- (2) In order to prove the convergence, the switching function σ_t has been included in the control algorithm and the following assumption has been stated

$$U_{\max} \geq \frac{\mu^* V_{\max}}{V_{\min} - S^*}.$$

It is worth noting that these precautions were omitted in the simulation results presented above, since U_{\max} was arbitrarily fixed at 0.39 and the switching function σ_t was not used in practice. These are necessary to prove the theoretical results but appear to be usually inoperative in the simulation experiments.